Open access • Journal Article • DOI:10.1016/J.SNB.2016.08.080

Ultrasensitive WO3 gas sensors for NO2 detection in air and low oxygen environment — Source link

Barbara Urasinska-Wojcik, Timothy A. Vincent, M.F. Chowdhury, Julian W. Gardner

Institutions: University of Warwick

Published on: 01 Feb 2017 - Sensors and Actuators B-chemical (Elsevier Science SA)

Topics: Methane and Combustion

Ultrasensitive WO_3 gas sensors for NO_2 detection in air and low oxygen environment

Barbara Urasinska-Wojcik[a], Timothy A. Vincent[a], Mohamed F. Chowdhury[b], Julian W. Gardner[a,b,*]

[a] *University of Warwick, School of Engineering, Coventry, CV4 7AL, UK*
[b] *Cambridge CMOS Sensors, Deanland House, 160 Cowley Road, Cambridge, CB4 0DL, UK*

[*] *Corresponding author:* Tel.: Email address: J.W.Gardner@warwick.ac.uk

Abstract

We report here on the results of a study into the response of a tungsten oxide based low power MEMS gas sensor to ppb of nitrogen dioxide at low levels of ambient oxygen. It was found that the resistive gas sensors not only had a high sensitivity to NO_2 (3.4%/ppb vs. 0.2%/ppb obtained for commercial MOX) but can still operate reliably at lower oxygen levels (down to 0.5 %) albeit with slightly longer response and recovery times. The optimal operating temperature was determined to be ca. 350°C and so easily within the range of a MEMS based SOI CMOS substrate. The response was sensitive to significant changes in ambient humidity, but was found to have low cross-sensitivity to CO, hydrogen, methane, and acetone even at much higher ppm levels. We believe that these tungsten oxide gas sensors could be exploited in harsh applications, i.e. with a low oxygen (lean) environment often associated in the exhaust gases from combustion systems.

Keywords

Gas sensor, lean air, metal oxide, nitrogen dioxide

1. Introduction

The gas nitrogen dioxide (NO_2) is an increasing problem for air quality in our cities. The gas can cause various problems such as damage to our lungs, smog or acid rain and, is principally formed from the combustion of fossil fuels in internal combustion engines, along with other forms of NO_x such as NO and N_2O [1]. For example as little as 50 ppb can inflame the airways in lungs [2]. Several types of NO_x gas sensors have been developed and commercialised including metal oxide semiconductors and solid electrolytes [3-6]. Among metal oxide semiconductors, specifically those based on WO_3 are of particular interest due to their structural simplicity, high sensitivity, low cost and potential durability for operation under extreme conditions [7-9].

Nanostructured metal oxide semiconductors are widely used for the fabrication of sensors for the detection of both oxidising (such as NO_2) and reducing gases (such as CO) [10]. The sensitivity to gases arises from the formation of a depletion region on the boundary between the n-type semiconducting metal oxide grains according to the reaction with atmospheric oxygen that takes place above 100 °C [11, 12]:

$$\tfrac{1}{2}\, O_2 + e^- \rightleftarrows [O^-] \qquad (1)$$

The concentration of chemisorbed oxygen $[O^-]$ is believed to control directly the level of lattice defects and to relate to the concentration of free electrons that in turn controls the width of the depletion layer [7]. When an oxidising gas is introduced to an n-type semiconductor surface, the concentration of electrons on the surface decreases and the resistance of the n-type semiconductor increases. Since WO_3 is an n-type semiconductor like tin dioxide it means that NO_2 forms anionic adsorbates on the surface of WO_3 grains according to a schematic reaction:

$$R_{(gas)} + e^-_{(from\ surface)} \rightarrow R^- \qquad (2)$$

where R means the oxidising gas (e.g. NO_2) and R^- means the anionic adsorbate on the surface (e.g. NO_2^-).

Our work focuses on the detection of NO_2 when the partial pressure of oxygen is much less than ambient, in other words when there is a lean environment. This is often the case following a combustion process where most of the air is converted into CO_2. This

condition of low oxygen levels is one that has not been widely investigated for metal oxide gas sensors.

We have studied experimentally the response of WO_3 based CMOS gas sensors to ppb levels of NO_2 at different oxygen levels. We have also investigated the cross-sensitivity to other gases at much higher levels as well as ambient humidity. In addition, we ~~report~~compare the ~~results~~performance against~~s for the~~ commercial sensors (MiCS-2714 supplied by SGX Sensortech).

Recently SAW based NO/NO_2 sensor has been shown to detect down to 1 ppb but suffer from a high temperature sensitivity and higher cost to manufacture [13]. Furthermore room temperature sensing is generating much research interest, in particular combining MOX, CNT and graphene [14], but it generally suffers from slower response times, poor baseline stability, and high humidity dependence.

2. Material and Methods

2.1. DC measurements

The typical sensing method for semiconducting metal oxide gas sensors is the measurement of DC resistance or conductance. In this study, a low power MEMS based micro-hotplate gas sensor was used, and the operating temperature was controlled by an adjustable constant current circuit. The micro-hotplate is shown in Fig. 1(a) (CCS09C, Cambridge CMOS Sensors Ltd). The MEMS structure was fabricated in a commercial foundry and is based on silicon on insulator (SOI) technology [15]. In the membrane structure, a tungsten resistive micro-heater is embedded within a 5 μm thick metal/oxide stack ensuring a low DC power consumption (e.g. 65 mW at 600 °C). The membrane is fabricated via a post CMOS deep reactive ion etch (DRIE) and both mechanically supports and thermally isolates the heater from the sidewalls. The MEMS micro-hotplate can reach temperatures well in excess of 500 °C and has a sub-5V controlled temperature ramp capability of 30 ms heating time and 60 ms cooling time from ambient to 500 °C.

2.2.Sample preparation

WO_3 powder (New Metals and Chemicals Ltd.) was mixed with an organic dispersant ESL 400 to obtain a paste. The weight ratio of the powder and the organic dispersant was 1:2. The paste was drop caste onto the 1 mm by 1 mm silicon die, which consisted of gold interdigitated electrodes on top of the membrane as a single-chip solution (Figs. 1(a) and

1(b)). After deposition of the WO_3 paste the substrate was left to dry in air at room temperature for ~12 h followed by annealing at 450 °C for 1 h, and then at 350 °C for about 23 h under ambient air to obtain the sensor element consisting of n-type WO_3. Fig. 1 (c) shows a scanning electron micrograph of the annealed paste with a porous microstructure. Finally, the silicon die was wire-bonded onto a standard TO-46 header (Fig. 1 (d)).

Figure 1 near here

2.3. Gas tests

The gas sensing measurements were performed at the Microsensors and Bioelectronics Laboratory at the University of Warwick using fully-automated custom rig (Fig. 2). The CMOS micro-hotplate substrates mounted on TO46 packages were connected to a custom made printed circuit board. Both the micro-heater and chemiresistor were driven/measured using National Instruments DAQ hardware and software. The gas sensing properties of the sensor element were characterised using a flow type sensing measurements apparatus. The gas sensor was placed inside an aluminium sample chamber equipped with standard Swagelock^{TM} gas inlet and outlet connectors. Synthetic air or nitrogen was introduced into the sample chamber for 5 min and then a gas mixture of NO_2 in air was injected for 5 min in steps of varying concentrations of 250, 100, 50, 25 and 10 ppb. The total gas flow rate was 1.2 slpm and the measurements were performed at room temperature in dry conditions and then at 50% and 25% relative humidity (RH). A LabView (National Instruments) interface allowed fully automated control of the digital mass flow controllers of the gas testing system.

Figure 2 near here

3. Results and Discussion

3.1. Response for Detecting NO_2 in Air

In this work, the sensor response (S) is defined as the ratio R_{NO2}/R_{air} or R_{NO2}/R_{N2} where R_{air}, R_{NO2} and R_{N2} are the electrical resistance of the tungsten oxide in air, nitrogen dioxide and nitrogen, respectively. Initially the WO_3 based sensors were exposed to NO_2 at concentrations ranging from 10 to 250 ppb in 50% RH air; to obtain the optimum working temperature of the sensor, as shown in Fig. 3(a). The sensor response initially increased with increasing heater temperature and then gradually decreased with further increases in

temperature. The maximum sensor response S was found to be about +525% for 100 PPB at 300 °C. In addition, the response (t_{90}) and recovery (t_{10}) times were determined for 100 ppb of NO_2 at 300 °C (Fig. 3(b)) and found to be 40 s and 205 s, respectively and, significantly decreased with the increasing operating temperature. The response time ranged from 35 to 15 s and the recovery time from 84 to -29 s across the temperature range of 350 to 450 °C. It was decided to operate the sensor at the working temperature of 350°C rather than 300°C to enhance significantly the recovery time.

Figure 3 near here

The time-dependent resistance change of WO_3 laboratory sensors to NO_2 pulses in dry and 25% RH air is shown in Fig. 4(a). When NO_2 gas was introduced, the resistance of the WO_3 sensor element increased with increase in the concentration of NO_2. This is a typical response of an n-type oxide towards an oxidising gas, leading to $R_{NO2} > R_{air}$ (or R_{N2}). For comparison, commercial NO_2 sensors ~~models of~~ (SGX Sensortech ~~senso~~, ~~r (~~MiCS-2714) that consist of a metal oxide sensing layer were tested using the same gas concentrations and heating power 43 mW (Fig. 4(a)). The response of semiconductor metal oxide gas sensor is empirically represented by the following power law [11]:

$$S = 1 + A_g C_g^{\beta} \quad (3)$$

where A_g is a prefactor that depends on the type of the sensing material, the operating temperature, and the type of gas interacting with the sensor. C_g is the gas concentration and β is the exponent factor, and its ideal value of 0.5 or 1 depends on the charge state of surface oxygen species and the stoichiometry of the elementary reactions on the surface [16]. According to the above power law equation, the value of β from the experimentally measured response versus concentration plot (Fig. 4(b)) was 0.988. This value of β exponent is close to theoretical value of 1 suggesting that the chemisorbed surface oxygen species are nearly all in the O^- state. The responses at 10 ppb and 250 ppb are calculated to be 1.2 and 4.5, respectively (Fig. 4(b)). The sensitivity S' of a gas sensor is defined as the derivative of the response S to the gas concentration and in this study is presented in percentage and varies between 1.9 and 1.4 % ppb^{-1} for the concentration range 10-250 ppb.

Figure 4 near here

This sensor performance is ~~much~~significantly better compared to the results from the commercial sensors and also better than generally reported in the literature. For example, Akiyama *et al.* [1] fabricated a sintered WO_3 film which was found to be sensitive to 80 ppm NO_2 in air at 300 °C. Tamaki *et al.* [17] studied the effect of the grain size of WO_3 on the response of a sensor to NO_x. The crystallite size varied between 20 and 57 nm and the grains were most sensitive to target gases in 5-10 ppm range at 25 nm size. Cantalini *et al.* [18] also demonstrated sensitivity of the sensor based on thin WO_3 film to NO_2 gas between 0.7 and 5 ppm at 250 °C whereas thick-film sensors made by Chung *et al.* [19] using a screen printing method showed sensitivity to 100 pm NO_2 in air at 100°C. The commercial NO_2 sensors, tested alongside the WO_3 laboratory sensors, performed poorly by comparison. The devices did not produce a stable response over the duration of our experiments, regardless of RH condition. The significant baseline drift and slow response to NO_2 presence prevented the identification of concentrations less than 100 ppb.

In the past decade, WO_3 nanostructures with large surface-to-volume ratios have also been considered for gas sensing applications. Although they show high response to NO_2 in sub ppm range, they require the use of expensive and complicated synthetic methods such as thermal evaporation [20], vapour transport [21] and templating [22]. To the best of our knowledge, WO_3 sensors capable of measuring NO_2 in ppb range can be currently obtained using either screen-printed films of few tens of microns thick with very fine microstructure and large porosity [23] or nanowires structure of WO_3 directly grown onto MEMS hotplates by using chemical vapour deposition method [24].

In our sensors, the enhanced sensing properties are likely achieved due to the small grain size. The obtained surface of WO_3 grains becomes more reactive and likely to adsorb the oxygen and form ionised oxygen species. On the other hand, our several μm thick WO_3 active layer has a form of porous structure on the interdigitated electrodes and this enhances the diffusion of NO_2 in the sensing body and enables the process to reach the inner part of the film. The heat transfer should also be better in such kind of porous structures, so the temperature of the film should be uniform. Our initial experiments showed that the annealing temperatures did not show the effect on the sensor response, while the increase in the annealing time had positive effects on the sensitivity, cross sensitivity and long term stability properties.

3.2 Response for Detecting NO_2 in Low Oxygen Environment

Further NO_2 sensing experiments were carried out in low oxygen environment. The time-dependent resistance change to NO_2 pulses (100-10 ppb) in 25% RH N_2 with 0.5, 1 and 2 % of O_2 measured at 350 °C is shown in Fig. 5(a). Sensitivity at 100 ppb varied between 3.4 and 3.1 % ppb^{-1} for the O_2 concentration range 0.5 - 2%. The sensor response remained almost unchanged when exposed to NO_2 in 25% RH N_2 when 0.5 and 1% of O_2 was introduced, and did not significantly change at 2 % of O_2 (Figs. 5(a) and 5(b)). It was also observed that response and recovery times decreased with increasing O_2 levels in the gas concentration. The average response and recovery times were 37 s and 40 s respectively for 100 ppb of NO_2 and concentration of O_2 1 % and 2%. These values increased to 57 s (t_{90}) and 44 s (t_{10}) when the concentration of O_2 was lowered to 0.5 %. Fig. 5(c) presents the experimentally measured response vs. NO_2 concentration in N_2 with 0.5-2 % of O_2. A power law has been fitted through the experimental points and the value of β is close to unity in all cases suggesting that the chemisorbed oxygen species are in O^- state.

Figure 5 near here

Table 1 summarises the typical response *S* of the sensing element to NO_2 in 25% RH N_2 with 0.5, 1 and 2 % O_2 content. Laboratory ~~S~~sensors showed the highest response in N_2 with 1 % O_2 content and these responses were comparable to that obtained in air. Table 2 lists the corresponding sensor sensitivity *S'* values that are almost independent of gas concentration, because the power factor β has a value close to unity.

Table 1 near here

Table 2 near here

Further NO_2 sensing experiments were carried out in N_2 with 1 % O_2 content under the operating temperature range 250-450 °C. The effect of varying NO_2 concentration on the signal of WO_3 material under various temperatures is presented in Fig. 6(a). Films performing under the operating temperatures 350-450 °C showed fast response and recovery times (Figs. 6 (a) and (b)). The baseline of the sensor increased over time at 250 and 300 °C,

and the resistance of the film significantly increased suggesting a strong interaction between the sensing material and the target gas. The highest response was obtained at 300 °C (see Fig. 6(c) and Tables 3 and 4).

Figure 6 near here

Table 3 near here

Table 4 near here

Fig. 7 illustrates the comparison of the results of sensor responses measured in air and low oxygen environment where the operating temperature is varied. It is seen in both cases that the response goes through a maximum on changing temperature taking a volcano shape. This increase of response (between 250 and 300 °C) results from an increase on the rate of the surface reaction of the NO_2 target gas, while the decrease of response (from 300 to 450 °C) results from a decrease in the utility of the gas sensing body. At the temperature of the maximum response 300 °C, the target gas molecules have optimum reactivity for the diffusion in the whole sensing area and exert large interaction with the WO_3 surface.

Figure 7 near here

3.3 Sensing mechanism

In WO_3 like in the most semiconducting oxide based sensors, the change in resistance is primarily caused by the chemical adsorption and reaction of the gas molecules on the surface of the sensing material. The surface of oxide semiconductor can adsorb oxygen from the ambient atmosphere:

$$O_{2(gas)} \rightleftarrows O_{2(MOX\ surface)} \quad (4)$$

These chemisorbed oxygen species act as surface acceptors by trapping electrons and increasing the resistance of the metal oxides as follows:

$$O_{2(MOX\ surface)} + e^- \rightleftarrows O_2^-{}_{(MOX\ surface)} \qquad T < 100\ °C \qquad (5)$$

$$O_2^-{}_{(MOX\ surface)} + e^- \rightleftarrows 2O^-{}_{(MOX\ surface)} \qquad 100\ °C \leq T \leq 300\ °C \qquad (6)$$

$$O^-{}_{(MOX\ surface)} + e^- \rightleftarrows O^{2-}{}_{(MOX\ surface)} \qquad T > 300\ °C \qquad (7)$$

At low temperatures, a reversible oxidising interaction takes place and the predominant oxygen species on the surface of the sensors prevails as O_2^-. Based on previous studies [6, 7, 9], it is well known that the direct interaction of NO_2 molecules with O_2^- ions is unlikely and the molecules directly interact with surface W ions:

$$NO_2 + e^-{}_{(from\ WO3)} \rightarrow NO_2^-{}_{(WO3\ surface)} \qquad (8)$$

Reversal of the above reaction is unlikely but disintegration of the ionosorbed NO_2 species into NO and a surface ion is also possible- to occur [9, 25]:

$$NO_2^-{}_{(WO3\ surface)} \rightarrow NO_{(gas)} + O^-{}_{(WO3\ surface)} \qquad (9)$$

Although the above reaction was not observed in our experiments, the evidence of possible reaction was previously demonstrated by Arai *et al.* in the FTIR spectrum of adsorbed NO_2 on the Rh/Al_2O_3 catalyst [25].

In the temperature range 250-300°C the response time for the detection of NO_2 is significantly high: 100 s and 200 s for the experiments in air and low oxygen environment respectively (Figs. 3(b) and 6(b)). It has been shown [4, 9] that in this temperature range, the ionosorbed molecular oxygen O_2^- tend to dissociate into two independent atomic O^- ions:

$$O_2^-{}_{(WO3\ surface)} + e^-{}_{(from\ WO3)} \rightarrow O^-{}_{(WO3\ surface)} + O^-{}_{(WO3\ surface)} \qquad (10)$$

These ionosorbed molecular oxygen O_2^- ions compete with adsorbing NO_2 gas molecules for the available surface sites and electrons from the conduction band of WO_3. This process involves trapping of electrons into physisorbed O_2 or NO_2 surface species but not their re-

emission. This is the reason for the saturation observed in Fig. 7 as well as the asymmetry with respect to response and recovery times which is more prominent for the experiments in air (Figs. 3(b) and 6(b)).

As the surface temperature was further raised, the concentration of O^- ions on WO_3 surface increased. With significant amount of O^- ions being available on the surface, the following oxidation reaction is possible:

$$NO_{2(gas)} + O^-_{(WO3\ surface)} \rightarrow NO_{(gas)} + O_{2(gas)} + e^- \quad (11)$$

This kind of relation contributes to a reducing interaction as observed in the high temperature-low concentration regime (Figs. 6(a) and 7). Increasing temperature also induces desorption of the target gas. This explains why the response decreased drastically above the optimum operating temperature. Similar observations have also been demonstrated for other metal oxides towards NO_2 sensing [4].

Considering the above surface reactions and sensor responses we can state that the changes in the oxygen concentration in contrast with temperature, did not significantly affect the sensor performance. It is also worth to mention that NO_2 seems to be able to interconvert into different nitrogen containing species on the sensing layer. Limiting the oxygen concentration restricts the availability of surface oxygen ions and prevents the formation of other forms of NO_x.

3.4 Cross-sensitivity measurements

WO_3 sensors are known to be sensitive towards various oxidising and reducing gases. Hence some selectivity measurements have been performed and they are presented in Fig. 8. The sensors were also tested for cross-sensitivity in the presence of carbon monoxide, hydrogen sulphide, acetone, methane and hydrogen at various concentration ranges. As expected, the resistance of the sensing element decreased on exposure to reducing gases leading to response values defined as the inverse of before so R_{air} / R_{NO2}. Table 5 summarises the response of the sensing element to these other gases. The values show that the WO_3 material is not so sensitive to CO, acetone, CH_4 and H_2 but rather sensitive to H_2S. However, even the exposure to 5ppm H_2S is far less than that to 250 ppb NO_2.

Table 5 near here

Although the oxidising gases directly adsorb onto the oxide surface, the reducing gases react with oxygen to produce water molecules. It is well known that at typical sensor operating temperatures above 300 °C, the dominant species on oxide surface is O^- [26]. Upon interaction of adsorbing CO gas molecules with surface oxygen ions the following reaction is likely to take place:

$$CO_{(gas)} + O^-_{(WO3\ surface)} \rightarrow CO_{2(gas)} + e^- \quad (12)$$

This reaction donates an electron to the WO_3 conduction band thereby increasing the conductivity of the tungsten oxide. The closely similar behaviour of C_3H_6O, H_2S, H_2 and CH_4 suggest that these gas molecules also might undergo an oxidation reaction closely analogue to CO:

$$C_3H_6O_{(gas)} + 8O^-_{(WO3\ surface)} \rightarrow 3CO_{2(gas)} + 3H_2O_{(gas)} + 8e^- \quad (13)$$

$$H_2S_{(gas)} + 3O^-_{(WO3\ surface)} \rightarrow SO_{2(gas)} + H_2O_{(gas)} + 3e^- \quad (14)$$

$$H_{2(gas)} + O^-_{(WO3\ surface)} \rightarrow H_2O_{(gas)} + e^- \quad (15)$$

$$CH_{4(gas)} + 4O^-_{(WO3\ surface)} \rightarrow CO_{2(gas)} + 2H_2O_{(gas)} + 4e^- \quad (16)$$

The above reactions rely on the availability of atomic surface O^- ions and it is clear that they can only occur at those temperatures where the ions abound on the sensing material surface, above 300 °C.

In our experiments a reversible decrease of surface resistance in the presence of water was observed (Fig. 8). As semiconducting dry WO_3 is brought in contact with humid air, water molecules chemisorb on the available sites of the oxide surface. At the operating temperature range 250-450 °C, the adsorption of water molecules on the surface takes place via dissociative chemisorption processes which may be described as follow [27, 28]:

(i) Water molecules adsorbed on grain surface react with the lattice W as:

$$H_2O_{(WO3\ surface)} + O_o + W \rightleftarrows 2OH - W_{(WO3\ surface)} + V_o + 2e^- \quad (17)$$

where O_o is the lattice oxygen and V_o the vacancy created at the oxygen site according to:

$$O_o \rightleftarrows O^{2-} + V_o$$

(18)

(ii) Ionised oxygen displaced from the lattice reacts with H^+ from the dissociation of water molecules and forms hydroxyl group:

$$H^+ + O^{2-} \rightleftarrows OH^- \quad (19)$$

Tungsten oxide has electron vacancies were electrons are accumulated and consequently the resistance of the sensing element decreases with increase in relative humidity.

Figure 8 near here

4. Conclusions

In this study we report upon the response of a tungsten oxide based MEMS gas sensor to ppb levels of nitrogen dioxide under various operating conditions. The response was found to be excellent of *ca*. 500% to a 100 ppb pulse of NO_2 in air at 350°C. ~~and t~~This value is so much higher than that ~~when compared to the~~ obtained for the reference commercial sensors tested in our laboratory and also higher than reported elsewhere in the literature. Here, we believe for the first time, we report the response of the gas sensor at low oxygen levels (down below 1%) under different operating temperatures, ranging between 250 and 450°C. It was found that these sensors with the active layer prepared by drop casting and annealing work reliably at low oxygen levels with again a high gas sensitivity but with longer response and recovery times (20% or so). These low cost sensors unlike commercial MOX devices also showed superior stability throughout the gas concentration range studied in dry and humid air, low oxygen environment and operating temperatures between 350 and 450°C. Our comparative tests against commercially available devices demonstrate the significant improvement achieved with our MEMS sensors over the current generation. We also showed that there was a small sensitivity to changes in humidity (ca. 0.2%/%RH) but a negligible cross-sensitivity to CO, H_2, CH_4 and acetone at much higher ppm levels. In conclusion, we believe that this MEMS based semiconducting gas sensor can be used to detect ppb levels NO_2 under the harsh conditions of low oxygen levels and high CO levels. Consequently, this low cost

MEMS sensor could find application in the detection of NO_2 in the exhaust gases from combustion systems such as car engines or gas boilers.

Acknowledgements

This work was fully supported by the EPSRC project: EP/L018330/1.

References

1. M. Akiyama, J.Tamaki, N. Miura, N. Yamazoe, Tungsten oxide-based semiconductor sensor highly sensitive to NO and NO_2, Chemistry Letters (1991) 1611-1614.
2. The National Institute for Occupational Safety and Health (NIOSH) http://www.cdc.gov/niosh/idlh/10102440.html, (accessed 09.05.16).
3. Z. Ling, C. Leach, R. Freer, A time resolved study of the response of a WO_3 gas sensor to NO_2 using AC impedance spectroscopy, Sensors and Actuators B, 87 (2002) 215-221.
4. B. Ruhland, T. Becker, G. Muller, Gas-kinetic interactions of nitrous oxides with SnO_2 surfaces. Sensors and Actuators B, 50 (1998) 85-94.
5. G.F. Fine, L.M. Cavanagh, A. Afonja, R. Binions, Metal Oxide Semi-Conductor Gas Sensors in Environmental Monitoring, Sensors 10 (2010) 5469-5502.
6. L. You, F.Y., X. He, Y. Sun, G. Lu, Highly sensitive NO_2 sensor based on monodispersed WO_3 nanoparticles, in 14th International Meeting on Chemical Sensors - IMCS 2012, Nürnberg/Nuremberg, Germany, 2012, pp. 1081-1084.
7. N. Yamazoe, G. Sakai, K. Shimanoe, Oxide semiconductor gas sensor, Catalysis Surveys from Asia 7 (2003) 63-75.
8. T. Akamatsu, T. Itoh, N. Izu, W. Shin, NO and NO_2 sensing properties of WO_3 and Co_3O_4 based gas sensors, Sensors 13 (2013) 12467-12481.
9. G. Chandrasekaran, A. Sundararaj, H.A. Therese, K. Jeganathan, Ni-catalysed WO_3 nanostructures grown by electron beam rapid thermal annealing for NO_2 gas sensing, Journal of Nanoparticle Research 17 (2015) 1-11.
10. N.P. Zaretskiy, L. I. Menshikov, A. A. Vasiliev, Theory of gas sensitivity of nanostructured MOX layers: Charge carrier self-exhaustion approach, Sensors and Actuators B 175 (2012) 234-245.
11. J.W. Gardner, Electrical conduction in solid-state gas sensors, Sensors and Actuators 18 (1989) 373-387.
12. J.W. Gardner, Detection of vapours and odours from a multisensor array using pattern recognition Part 1. Principal component and cluster analysis, Sensors and Actuators B 4 (1991) 109-115.
13. S.H. Wang , C.Y. Shen, J.M. Su, S.W. Chang, A room temperature nitric oxide gas sensor based on a copper-ion-doped polyaniline/tungsten oxide nanocomposite, Sensors 15 *(*2015) 7084-7095.
14. S. Liua, Z. Wanga, Y. Zhanga, C. Zhanga, T. Zhanga, High performance room temperature NO_2 sensors based on reduced graphene oxide-multiwalled carbon nanotubes-tin oxide nanoparticles hybrids, Sensors and Actuators B 211 (2015) 318–324.
15. S.Z. Ali, F. Udrea, W.I. Milne, J.W. Gardner, Tungsten-based SOI microhotplates for smart gas sensors, Journal of Microelectromechanical Systems 17 (2008) 1408-1417.
16. S. Santra, A. De Luca., S. Bhaumik, S.Z. Ali, F. Udrea, J.W. Gardner, S.K. Ray, P.K. Guha, Dip pen 1 nanolithography-deposited zinc oxide nanorods on a CMOS MEMS platform for ethanol sensing, RSC Advances 5 (2015) 47609-47616.
17. J. Tamaki, Z. Zhang, K. Fujimori, M. Akiyama, T. Harada, N. Miura, N. Yamazoe, Grain-size effects in tungsten oxide-based sensor for nitrogen oxides, Journal of the Electrochemical Society 141 (1994) 2207-2210.

18. C Cantalini, M.Pelino, H.T. Sunb, M. Faccioc, S. Santuccid, L. Lozzi, M. Passacantando, Cross sensitivity and stability of NO_2 sensors from WO_3 thin film, Sensors and Actuators B 35 (1996) 112-118.
19. Y.K. Chung, M.H. Kim, W.S. Um, H.S. Lee, J.K. Song, S.C. Choi, K.M. Yi, M.J. Lee, K.W. Chung, Gas sensing properties of WO_3 thick film for NO_2 gas dependent on process condition, Sensors and Actuators B 60 (1999) 49-56.
20. C.C. Liao, F.R. Chen, J.J. Kai, WO_{3-x} nanowires based electrochromic devices, Solar Energy Materials & Solar Cells 90 (2006) 1147-1155.
21. D. Meng, N.M. Shaalan, T. Yamazaki, T. Kikuta, Preparation of tungsten oxide nanowires and their application to NO_2 sensing, Sensors and Actuators B 169 (2012) 113-120.
22. K. Zhu, H. He, S. Xie, X. Zhang, W. Zhou, S. Jin, B. Yue, Crystalline WO_3 nanowires synthesized by templating method, Chemical Physics Letters 377 (2003) 317-321.
23. D.E Williams, J. Salmond, G.S. Henshaw, Y. Fai, D.B. Wells, G. Ding, J. Wagner, B. Wright, J. Wilson, Y.F. Yung, J. Akaji, G. Laing, Development of low-cost ozone and nitrogen dioxide measurement instruments suitable for use in an air quality monitoring network, ECS Transactions 19 (2009) 251-254.
24. F.E. Annanouch, Z. Haddi, S. Vallejos, P. Umek, P. Guttmann, C. Bittencourt, E. Llobet, Aerosol-assisted CVD-grown WO_3 nanoneedles decorated withcopper oxide nanoparticles for the selective and humidity-resilient detection of H_2S, ACS Applied Materials and Interfaces 7 (2015) 6842-6851.
25. H. Arai, H. Tominaga, An infrared study of nitric oxide adsorbed on rhodium-alumina catalyst, Journal of Catalysis 43 (1976) 131-142.
26. D.E. Williams, Conduction and gas sensor response of semiconductor gas sensors, in: Solid State Gas Sensors, P. T Moseley, B.C. Tofield (Eds.) Adam Hilger, Bristol, 1987, pp. 71-123.
27. N.K. Pandey, K. Tiwari, A. Roy, A. Mishra, A. Govindan, Ag-loaded WO_3 ceramic nanomaterials: characterization and moisture sensing studies, International Journal of Applied Ceramic Technolology 10 (2012) 150-159.
28. R. Azimirad, N.Naseri, O. Akhavan, A.Z. Moshfegh, Hydrophilicity variation of WO_3 thin films with annealing temperature, Journal of Physics D: Applied Physics 40 (2007) 1134-1137.

Tables

Table 1
Typical response (R_{NO2}/R_{N2} or R_{NO2}/R_{air}) of commercial MOX (MiCS-2714) sensor to NO_2 in air and laboratory WO_3 based sensor to NO_2 in air and N_2 pulses with O_2 concentration ranging from 0.5 to 2%. Measurements of were performed in 25% RH air or nitrogen.

NO_2 concentration [ppb]	**250**	**100**	**50**	**25**	**10**
Response at 0.5% O_2	-	4.3	2.7	1.8	1.3
Response at 1% O_2	-	4.5	2.7	1.8	1.3
Response at 2% O_2	-	4.1	2.5	1.7	1.4
Response in Air	4.5	2.6	1.8	1.4	1.2
Response in Air–MiCS-2714	1.5	1.2	1.1	1.0	1.0

Table 2
Sensitivity ($(R_{NO2}-R_{air}/R_{air})/c_{gas}$ or $(R_{NO2}-R_{N2}/R_{N2})/c_{gas}$) of commercial MOX (MiCS-2714) sensor to NO_2 in air and laboratory WO_3 based sensor to NO_2 in air and N_2 pulses with O_2 concentration ranging from 0.5 to 2%, (25% RH, 350°C).

NO_2 concentration [ppb]	250	100	50	25	10
Sensitivity at 0.5% O_2 [% ppb^{-1}]	-	3.3	3.4	3.1	2.9
Sensitivity at 1% O_2 [% ppb^{-1}]	-	3.4	3.4	3.1	2.5
Sensitivity at 2% O_2[% ppb^{-1}]	-	3.1	3.0	2.8	2.6
Sensitivity in Air [% ppb^{-1}]	1.4	1.6	1.6	1.6	1.9
Sensitivity in Air–MiCS-2714	0.2	0.2	0.2	0.2	0.2

Table 3
Typical response (R_{NO2}/R_{N2}) of WO_3 based sensor to NO_2 in dry N_2 pulses with 1% O_2 concentration and operating temperature ranging from 250 to 450 °C.

NO_2 concentration [ppb]	**100**	**50**	**25**	**10**
Response at 250°C	4.8	3.4	2.2	1.4
Response at 300°C	13.5	9.4	5.7	3.7
Response at 350°C	6.5	4.7	3.2	1.8
Response at 400°C	3.8	3.2	2.1	1.5
Response at 450°C	2.5	1.9	1.5	1.1

Table 4
Sensitivity ($(R_{NO2}-R_{N2}/R_{N2})/c_{gas}$) of WO_3 based sensor to NO_2 in N_2 pulses with 1% O_2 concentration and operating temperature ranging from 250 to 450 °C.

NO_2 concentration [ppb]	100	50	25	10
Sensitivity at 250°C [% ppb^{-1}]	4.5	4.8	4.6	4.6
Sensitivity at 300°C [% ppb^{-1}]	14.2	16.9	19.0	25.2
Sensitivity at 350°C [% ppb^{-1}]	6.5	7.4	8.6	8.4
Sensitivity at 400°C [% ppb^{-1}]	3.7	4.4	4.3	5.4
Sensitivity at 450°C [% ppb^{-1}]	1.8	1.8	1.7	1.1

Table 5
Response (R_{gas}/R_{air} or R_{air}/R_{gas}) of WO_3 based sensors to various gases at maximum concentration (operating temperature 350°C).

Gas	**CO**	**C_3H_6O**	**H_2S**	**H_2**	**CH_4**	**NO_2**
Concentration [ppm]	50	300	5	20000	15000	0.25
Response	1.6	2.3	3.3	1.0	1.0	4.5

Figure(s)

Figures

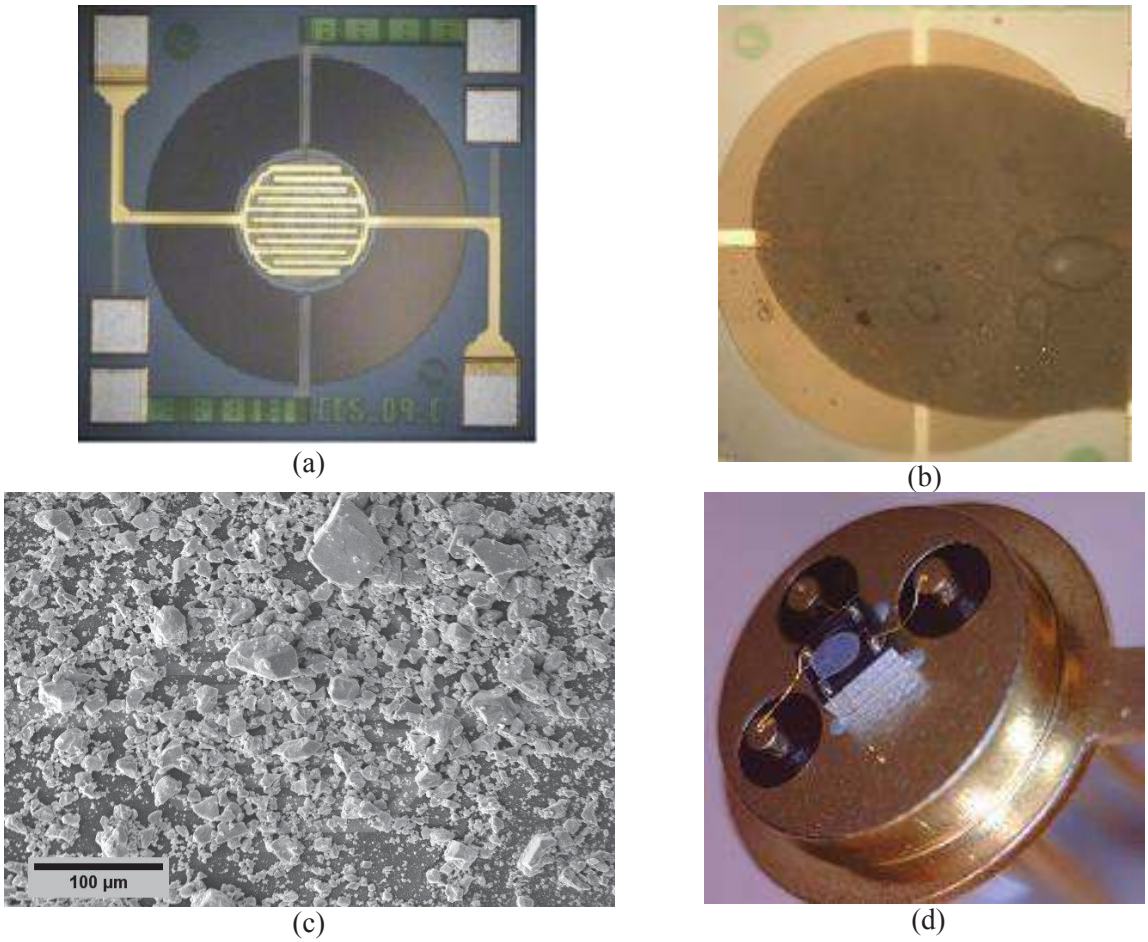

Fig.1. (a) Optical micrograph of a bare micro-hotplate (CCS09C, Cambridge CMOS Sensors Ltd). (b) Optical micrograph of a typical device after deposition of the WO_3 paste. (c) Scanning electron micrograph (250× magnification) of the surface of the deposited material. (d) Optical micrograph of a bonded micro-hotplate on a TO46 package.

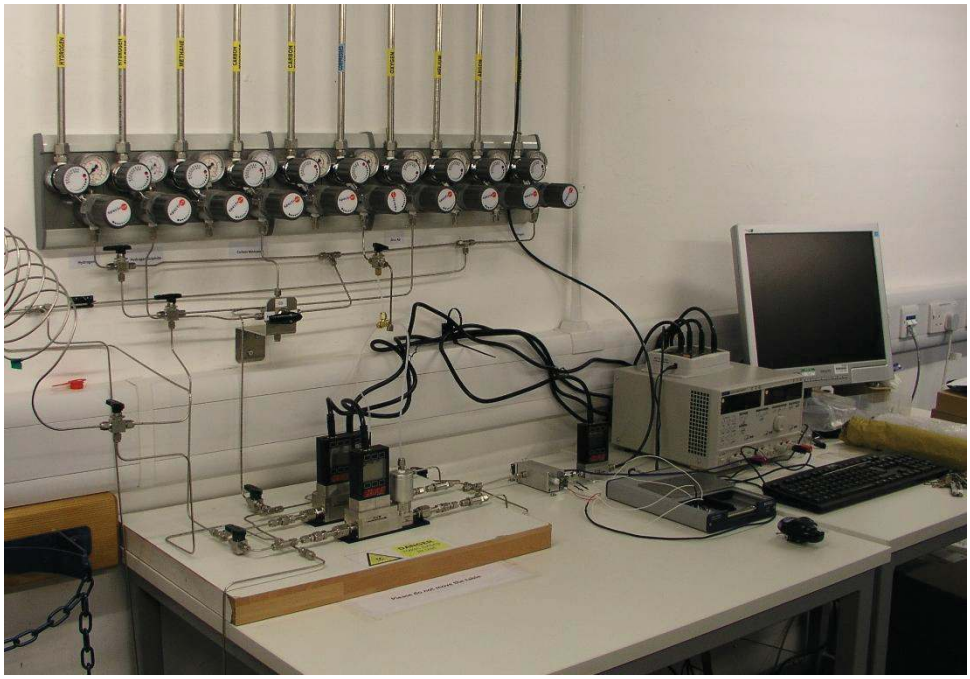

Fig.2. Photograph of the fully-automated custom designed gas testing rig. Precise gas mixtures in the ppb to percent range were generated using two mass flow controllers.

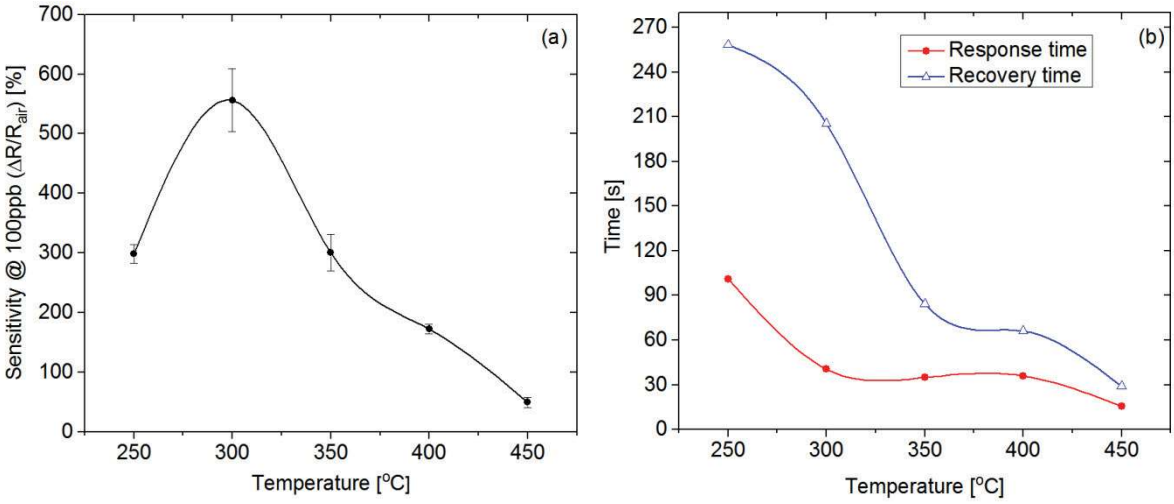

Fig.3. (a) Average sensor response as a function of temperature for 100 ppb of NO_2 in 50% RH air. The error bars represent the standard deviation of two measurements performed on separate sensors. (b) Response and recovery time at 100 ppb of NO_2 in 50% RH vs. temperature.

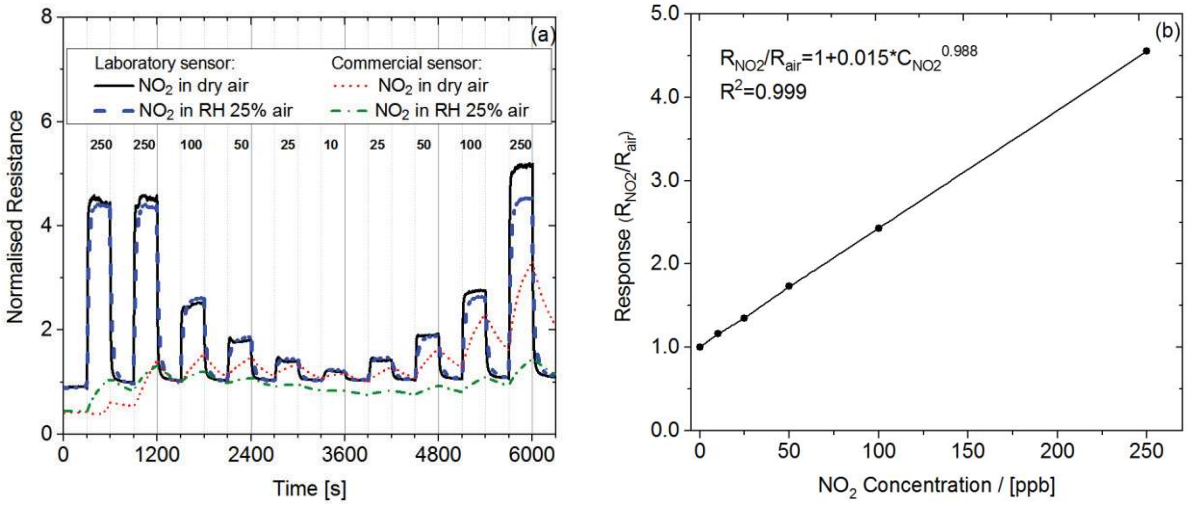

Fig.4. (a) Typical dynamic responses of laboratory WO_3 based sensor and commercial MOX (SGX Sensortech) sensor in presence of NO_2 (250-10 ppb) in dry and 25% RH air. (b) Response of the laboratory sensor as a function of concentration plot. Solid line represents the power law fitted through the experimental points.

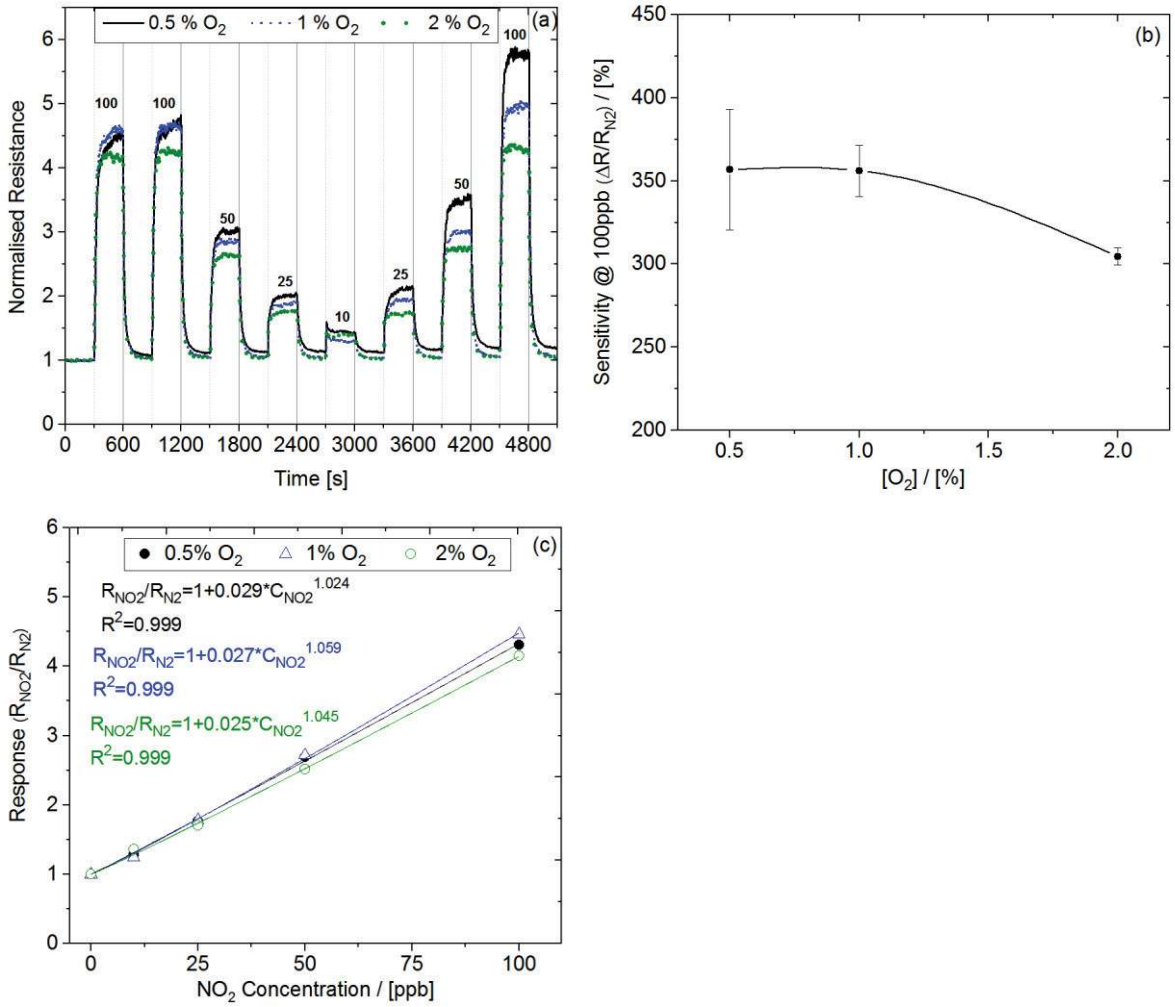

Fig.5. (a) Typical dynamic response of WO_3 based sensors exposed to NO_2 (100-10 ppb) in N_2 pulses at 25 % RH and 350°C, with O_2 concentration ranging from 0.5 to 2 %. (b) Response of the sensors at 100 ppb as a function of O_2 concentration plot. The error bars represent the standard deviation of two measurements performed on separate sensors. (c) Response of the sensors as a function of concentration plot. Solid line represents the power law fitted through the experimental points.

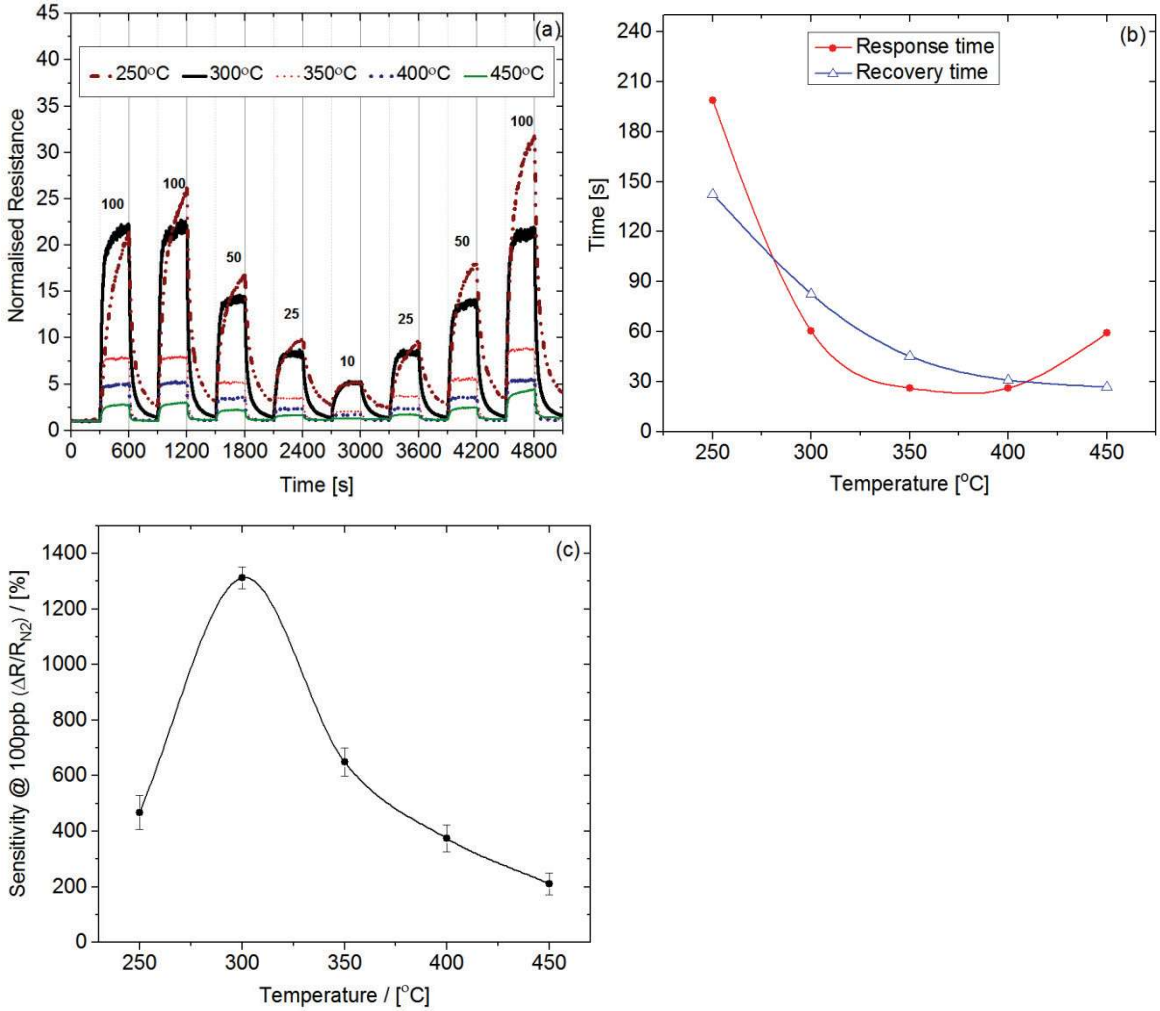

Fig.6. (a) Typical dynamic response of WO_3 based sensor exposed to NO_2 (100-10 ppb) in dry N_2 pulses with 1 % O_2 with temperature ranging from 300 to 400 °C. (b) Response and recovery time at 100 ppb of NO_2 in dry N_2 pulses with 1 % O_2 vs. temperature. (c) Response of the sensors at 100 ppb as a function of working temperature plot. The error bars represent the standard deviation of two measurements performed on separate sensors.

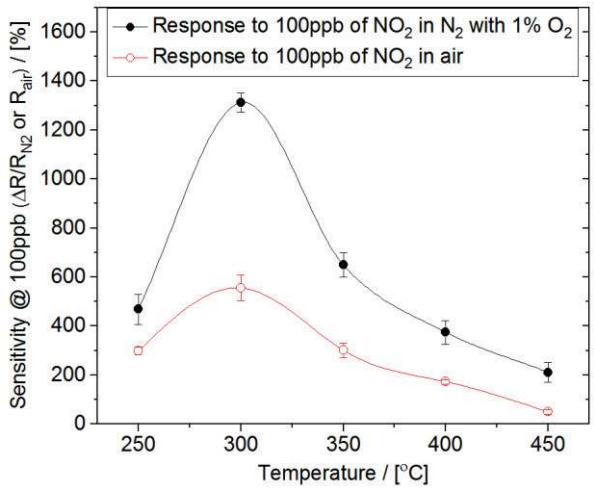

Fig. 7. Dependence of sensor response to 100ppb of NO_2 in N_2 with 1% O2 content and air on temperature.

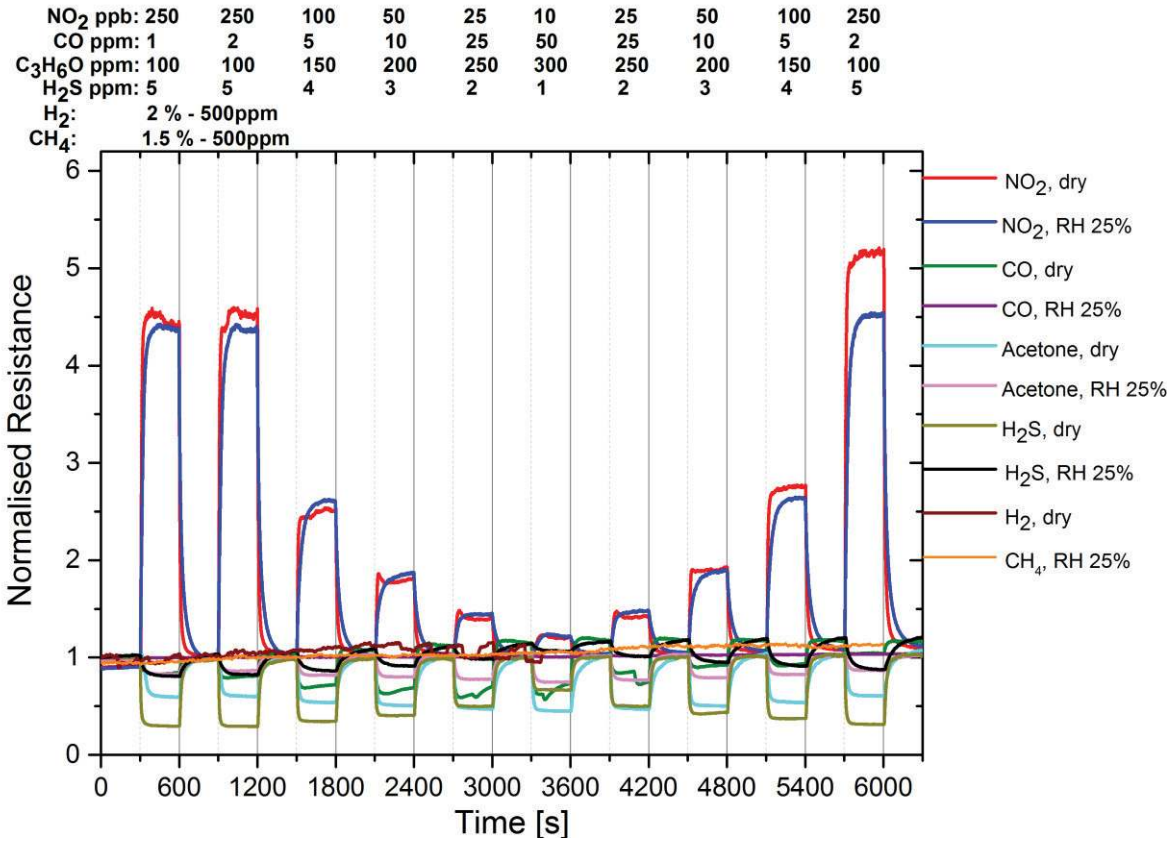

Fig. 8. Selectivity measurements of WO_3 based sensor exposed to CO (1-50 ppm), acetone (100-300 ppm), H_2S (1-5 ppm), H_2 (500 ppm-2 %) and CH_4 (500 ppm-1.5 %) in air.

Biographies

Barbara Urasinska-Wojcik MSc PhD is a research fellow in the Microsensors and Bioelectronics Laboratory at the School of Engineering, University of Warwick. Her research is currently focused on CMOS based chemical sensors. She previously was a part of the Knowledge Centre for Materials Chemistry (KCMC) at the University of Manchester and was working on fabrication and characterisation a range of organic semiconductor devices mainly OPVs and OFETs for liquid and vapour sensing. She also worked as a Postdoctoral Research Officer within the College of Physical and Applied Sciences at Bangor University. Her research involved organic photovoltaic materials, electrical and optical characterisation of organised molecular films and single molecule electronics. Her Ph.D. research was primarily focused on the design, preparation and characterisation of molecular diodes from new types of organic junctions, and also the electrical characterisation of molecular wires. She has published a number of technical papers focusing on molecular electronics, organised molecular films and organic semiconductor devices and their application in chemical and biological sensors.

Timothy Vincent is a PhD student at the University of Warwick, where he graduated with a first class degree in electronic engineering in 2013. His research interests include breath analysis, NDIR gas sensing and development of gas sensors for miniature systems. His work focuses on development of sensors systems for health care monitoring for point of care applications. He specialises in investigating the contents of breath and detecting VOCs in relation to metabolism and well-being monitoring.

M Foysol Chowdhury BSc MSc PhD MIET is the Director of R & D Projects at Cambridge CMOS Sensors Ltd (CCS). Soon after CCS was formed he joined the company as a Business Development Manager in 2009 where he played a critical role in early stage technology and business development phases. Previously, he was a Technical Lead, at another Cambridge University spin-off company (CamSemi), where he was responsible for chip assembly and signing off the mixed-signal ASIC chip development that was successfully launched for switch mode power supply controller applications to generate company's first revenues. He has more than 20+ years industrial experience in integrated circuits designs gained from Marconi Defence Systems, LSI Logic, Micron Technology Inc.. He held a number of post-doctoral fellowships at several UK universities working on leading-edge sensing solutions. His research interests are in MEMS, CMOS incorporating nanomaterial for sensing applications leading to Internet of Things, with specific expertise in environmental monitoring including health and wellbeing applications.

Julian W. Gardner BSc PhD DSc FIET FREng is the Professor of Electronic Engineering at the University of Warwick, UK. He has published over 450 technical papers and is an author of 8 books. He was an Alexander von Humboldt Fellowship in Germany in 1994 and Fellow of the Institute of

Technology in 1997. In addition to being professor of electronic engineering, he is Founder and Head of the Microsensors & Bioelectronics Laboratory; and co-director of the Centre for Cognitive & Neural Systems at Warwick. He was elected a Fellow of the Royal Academy of Engineering in 2006 and won the IET JJ Thompson Medal for Achievements in Electronics in 2007. He has been involved in the spin-out of three companies, with the latest "Cambridge CMOS Sensors Ltd" awarded Company of the Year in 2012 and 2015 at the Business Weekly Awards. His research interests are Microsensors & MEMS in general, and in particular Artificial Olfaction, Chemical Sensing, Smart Sensors**,** and Signal Processing Methods.